Noninvasive Bioluminescent and MicroPET Imaging for the Regulation of NF-κB in Human Hepatoma-bearing Mice

TSUI-JUNG CHANG[1], YA-JEN CHANG[1], TIN-YUN HO[2], CHIEN-YUN HSIANG[3], CHIA-YU YU[1], TE-WEI LEE[1], WU-JYH LIN[1] and CHIH-HSIEN CHANG[1]

[1]*Institute of Nuclear Energy Research, Taoyuan;*
[2]*Graduate Institute of Chinese Medical Science, and* [3]*Department of Microbiology, China Medical University, Taichung, Taiwan, R.O.C.*

Abstract. *The activity of nuclear factor-κB (NF-κB), a nuclear transcription factor, influences both critical tumor promotion and host–tumor interactions. Preventing NF-κB activation may thus inhibit the development of cancer. Therefore, development of easy and rapid methods to evaluate the regulation of NF-κB is needed for drug discovery. The aim of this study was to visualize the regulation of NF-κB by real-time, noninvasive bioluminescence and microPET imaging in vivo. Materials and Methods: A highly responsive HepG2/NF-κB/luc clone L for 12-O-tetradecanoylphorbol-13-acetate (TPA)-induced tumor promotion inhibited by methotrexate (MTX) was selected by high-throughput bioluminescent imaging (BLI) in vitro. BLI and microPET using ^{18}F-fluoro-deoxyglucose (FDG) imaging were performed in HepG2/NF-κB/Luc/L hepatoma-bearing SCID mice. Results: The luciferase expression by BLI assay reflected that the TPA-induced NF-κB activity was suppressed by MTX after 16 h treatment. A positive correlation between in vitro and in vivo MTX-suppressed TPA-induced NF-κB activity was indicated. MicroPET imaging could not demonstrate any decrease in FDG uptake during the early stage at 24 h after TPA and MTX treatment. Conclusion: BLI directly revealed that MTX inhibited cellular transformation by suppressing NF-κB activity. Molecular imaging would accelerate the validation of the gene regulation of tumor cells in preclinical cellular and mouse models.*

Correspondence to: Dr. Chih-Hsien Chang, Isotope Application Division, Institute of Nuclear Energy Research, 1000 Wenhua Road, Chiaan Village, Lungtan, Taoyuan 325, Taiwan, R.O.C. Tel: +88 634711400 ext 7227, Fax: +88634713491, e-mail: chchang@iner.gov.tw

Key Words: Bioluminescent imaging, ^{18}F-fluorodeoxyglucose, luciferase, micropositron-emission tomography (microPET), nuclear factor-κB.

Hepatocellular carcinoma (HCC), the third leading cause of cancer mortality in the world, usually develops in the background of chronic hepatitis with inflammation (1). The molecular and cellular mechanisms linking chronic inflammation to tumorigenesis remain unresolved. The activation of nuclear factor-κB (NF-κB), a hallmark of inflammatory responses that is usually detected in tumors, may constitute a missing link between inflammation and cancer. Intermittent suppression of a major signal factor, such as NF-κB, could be a useful tool to prolong the premalignant phase and inhibit tumor progression in chronic inflammatory diseases with high cancer risk (2, 3).

NF-κB is a nuclear transcription factor that affects a variety of cellular functions and influences tumor biology and host–tumor interactions. Heterodimers of NF-κB are most often sequestered in the cytoplasm in an inactive form bound to inhibitors of NF-κB (IκBs). When activated by a number of tumor-promoting agents, including tumor-necrosis factor-α (TNF-α), NF-κB binds to the NF-κB-responsive element present in the promoter of tumor-associated genes, leading to the induction of genes which then transforms hepatocytes into malignant cells (2, 4). Selective deletion or suppression of NF-κB activity could induce programmed cell death of transformed hepatocytes and subsequently reduce the incidence of liver tumors (1). Thus, preventing NF-κB activation in the hepatocytes of chronic liver inflammation may inhibit the development of liver cancer and is therefore a potential target for cancer prevention in chronic inflammatory diseases (1).

A wide range of human disorders involves inappropriate regulation of NF-κB, including cancer (5, 6), neurode-generative diseases (7), rheumatoid arthritis (8), asthma (9), inflammatory bowel disease (10) and atherogenesis (11). As treatments of such diseases may include selective modulators of NF-κB, it is necessary to validate these studies with appropriate animal models. Traditionally, NF-κB activity has been assessed in sacrificed animals by band-shift analysis of nuclear extracts, nuclear localization of NF-κB by specific

antibodies, or by analyzing reporter gene activity in homogenates (12) or sections (13) of transgenic mice containing a reporter gene controlled by NF-κB-responsive elements. Since phosphorylation of NF-κB in many cases is a prerequisite for transcriptional activity, nuclear localization or DNA binding alone cannot distinguish between transcriptionally active and inactive NF-κB (14). Furthermore, the sacrifice of mice is necessary for obtaining tissues in histological and cellular analysis. These methods take samples from living animals and sample preparations for detection are time consuming and tedious. In addition, these methods cannot easily reflect the real-time regulation of tumor promoting responses.

Noninvasive imaging of reporter gene expression using various imaging modalities is playing an increasingly important role in defining molecular events in the field of oncology. Bioluminescent imaging (BLI) provides sensitive *in vivo* detection and quantification of cells specifically engineered to emit visible light (15). Nowadays, the development of transgenic mice provides a noninvasive model to define mechanisms through which NF-κB leads to the development of diseases (16-18). It is also very helpful to develop tumor-bearing mice that express a luciferase reporter whose transcription is dependent on NF-κB activity. The relative amount of luminescence can thus be assayed noninvasively by real-time imaging.

Functional positron-emission tomography (PET) using ^{18}F-fluorodeoxyglucose (FDG), which detects glucose metabolic activity, has been widely used to assess the location(s) of tumors for diagnosis and monitoring for recurrence or response to various treatments (19). Molecular imaging using microPET could monitor the genetic and cellular processes *in vivo* and provides a new era for many kinds of research in small animal studies (20, 21). A multimodality approach combining BLI and nuclear imaging would provide the advantages of speed and ease of validating gene regulation and metabolism in tumor cells.

12-*O*-tetradecanoylphorbol-13-acetate (TPA) is a potent tumor promoter and shares several biological activities of epidermal growth factor (EGF) (22). Study of antitumor promotion by cancer drugs and compounds has been utilized in TPA- induced tumor promotion models (23, 24). Although the role of NF-κB in tumor promotion and suppression has been discussed, direct visualization of NF-κB regulation by methotrexate (MTX) and simultaneous monitoring of the glucose metabolism during MTX treatment in human hepatoma cells have not yet been reported. In this study, a human hepatoma stable clone (HepG2/NF-κB/Luc/L) transfected with a luciferase gene driven by NF-κB-responsive elements was constructed and selected. The regulation of NF-κB by MTX on the TPA-induced-tumor promotion was monitored by bioluminescent imaging (BLI) *in vitro*. Furthermore, the regulation of NF-κB and glucose uptake by MTX was evaluated by BLI and FDG/microPET noninvasive imaging in HepG2/NF-κB/Luc/L hepatoma-bearing SCID mice.

Materials and Methods

Cell culture and stable transfection. HepG2 cells were purchased from American Tissue Culture Collection (ATCC), and maintained in Dulbecco's modified Eagle's medium (DMEM) supplemented with 10% fetal bovine serum (FBS) and 400 μg/ml G-418 (Life Technologies, Gaithersburg, MD, USA). Recombinant HepG2/NF-κB cells were co-transfected with AlwNI-linearized pNF-κB-Luc DNA containing five NF-κB responsive elements (5'-TGGGGACT TTCCGC-3') upstream of a firefly luciferase gene (Stratagene, La Jolla, CA, USA) and 2.5 μg EcoRI-linearized pSV3-neo DNA by SuperFect transfection reagent (Qiagen, Valencia, CA, USA). Diluted single-cell clones were subcultured 48 h later and selected with 400 μg/ml G-418 (Promega, Madison, WI, USA) in 96-well plates. Recombinant bioluminescent cell clones were designated as HepG2/NF-κB/Luc (Figure 1).

TPA and MTX treatment. Single tumor clones were imaged and evaluated for stable bioluminescence activity *in vitro*. The TPA-induced highest expression single clones were selected for further animal experiments. Hepatoma cell lines (HepG2, HepG2/NF-κB/Luc clones) were seeded at a density of 5×10^3/100 μl in 96-well plates and allowed to adhere for 16 h at 37˚C. The cells were then treated with different amounts of TPA (20, 100 ng/ml) (Sigma, St. Louis, MO, USA) and methotrexate (10, 50, 100 μg/ml) and then incubated at 37˚C. After 16 h of incubation, the cells were washed with ice-cold PBS.

Luciferase activity imaging. The luciferase activity was measured by adding 200 μl luciferase reagents (150 μg/ml) (Xenogen, Alameda, CA, USA) for 10 min prior to imaging. Bioluminescent imaging was performed with a highly sensitive, cooled CCD camera mounted in a light-tight specimen box (IVIS® Imaging System 100 Series; Xenogen, USA), using protocols similar to those described elsewhere (15). Quantification of signals in the regions of interest (ROI) from displayed images were designated around each well by grid mode and quantified as total photon counts or photons/s using Living Image® software (Xenogen). Background bioluminescence from the imaging box was in the range of 1×10^4 photon counts or $1–2\times10^5$ photons/s.

WST-1 assay. Cell viability was quantified by colorimetry based on the metabolic cleavage of the tetrazolium salt WST-1 (Roche, Nutley, USA) by mitochondrial dehydrogenase in viable cells (25). After incubation for 16 h, 100 μl WST-1 reagent was added to each well and the plates were incubated for 2 h at 37˚C, at which time the absorbance of each well was measured at 450 nm with reference to 620 nm using a microplate reader (Thermo Labsystems, Beverly, MA, USA).

Animal experiments. Animal experiments were approved by the Institutional Animal Care and Use Committee (IACUC) of the INER. Twenty-one eight-week-old female SCID nu/nu mice obtained from the National Animal Center of Taiwan (Taipei, Taiwan) were subcutaneously injected with 1×10^6 HepG2/NF-κB/Luc/L cells in the right hind flank at day 0.

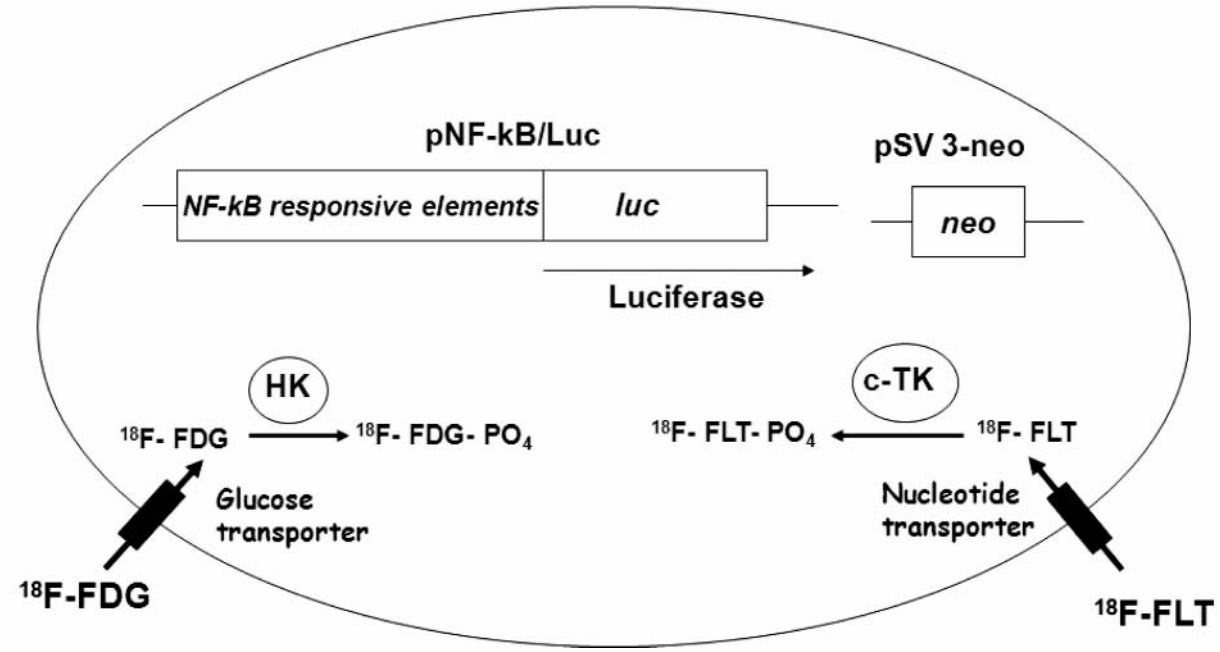

Figure 1. *Construction of HepG2/NF-κB/Luc cell lines for measuring reporter gene expression and glucose accumulation using different imaging modalities. Luc (firefly luciferase) is an optical bioluminescence reporter gene. ^{18}F-fluorodeoxyglucose (FDG) is a glucose metabolic PET imaging probe. Noninvasive, quantitative, and repeated imaging the luc gene expression either by catalysis of an optical reporter probe or by trapping of a PET probe can be imaged by both optical CCD camera and microPET in living subjects. HK: hexokinase; c-TK: cellular thymidine kinase; FLT: 3'-deoxy-3'-^{18}F-fluorothymidine.*

To monitor the treatment response, the mice were anesthetized with 1.5% isoflurane (positioned prone in the scanner) and performed BLI imaging on days 15 and 16 after tumor inoculation. Treatments were initiated when tumor volume was about 50 mm^3. Tumor volume was calculated as (length × width × height × 3.14)/6. The mice were divided into 3 experimental groups (n=5 at each group): The control (vehicle) group (Group A) was obtained by intraperitoneal treatment with phosphate-buffered saline (PBS). Group B was obtained by intraperitoneal treatment with TPA (0.5 mg/kg of TPA in 200 μl of PBS/mouse) on day 15 post inoculation of HepG2/NF-κB/Luc/L cells, and Group C was obtained by intraperitoneal treatment with TPA (0.5 mg/kg of TPA in 200 μl of PBS/mouse) and MTX (50 mg/kg) on day 15 post inoculation of HepG2/NF-κB/Luc/L cells.

In vivo imaging of luciferase activity. For *in vivo* BLI imaging, animals were anesthetized (1-2% isoflurane) and given the substrate D-luciferin intraperitoneally at 150 mg/kg in DPBS. At 10-15 min after luciferin injection, two mice were placed onto the stage inside the light-tight camera box with continuous exposure of 1-2% isoflurane and imaged with the IVIS Imaging System® 100 Series (Xenogen). Imaging times ranged from 2 s to 1 min, depending upon tumor bioluminescence and size. Regions of interest (ROI) from displayed images were designated around the tumor sites and quantified as total photons/s by the Living Image® software (Xenogen).

FDG/microPET imaging. The mice were divided into 3 experimental groups (n=2 at each group): Group A and B underwent the same treatments as described above. Group C was treated intraperitoneally with TPA (0.5 mg/kg of TPA in 200 μl of PBS/mouse) on day 15 and MTX (50 mg/kg) on day 16 post inoculation of HepG2/NF-κB/Luc/L cells. To monitor the treatment response of tumor, FDG/microPET scanning was performed on day 15 before treatment, and day 16 and 17 after tumor inoculation. The mice under gas anesthesia with isoflurane were injected *via* a tail vein with 250 μCi ^{18}F-FDG and then were imaged using a microPET-R4® system (Concorde Microsystems, Knoxville, TN, USA) (26). Only the data of 60-70 min after *i.v.* administration were reconstructed as static images. For data analysis, an ROI was placed on each tumor in the transaxial images. AsiPro software (Concorde Microsystems) was used for viewing microPET images and for data analysis. The counts in each ROI were converted to radioactivity per g of tissue (nCi/g), assuming a tissue density of 1 g/ml, and then normalized to percentage injected dose per gram of tissues (% ID/g).

Statistical analysis. Data are presented as mean±standard error (SE). Unpaired *t*-test was used for comparison between two experiments. A value of $p<0.05$ was considered statistically significant.

Results

Effect of TPA and MTX on the NF-κB activity in hepatoma cells. Since NF-κB is known to regulate cytokine and growth factor expression through binding to specific responsive elements located in the promoters of target genes, we

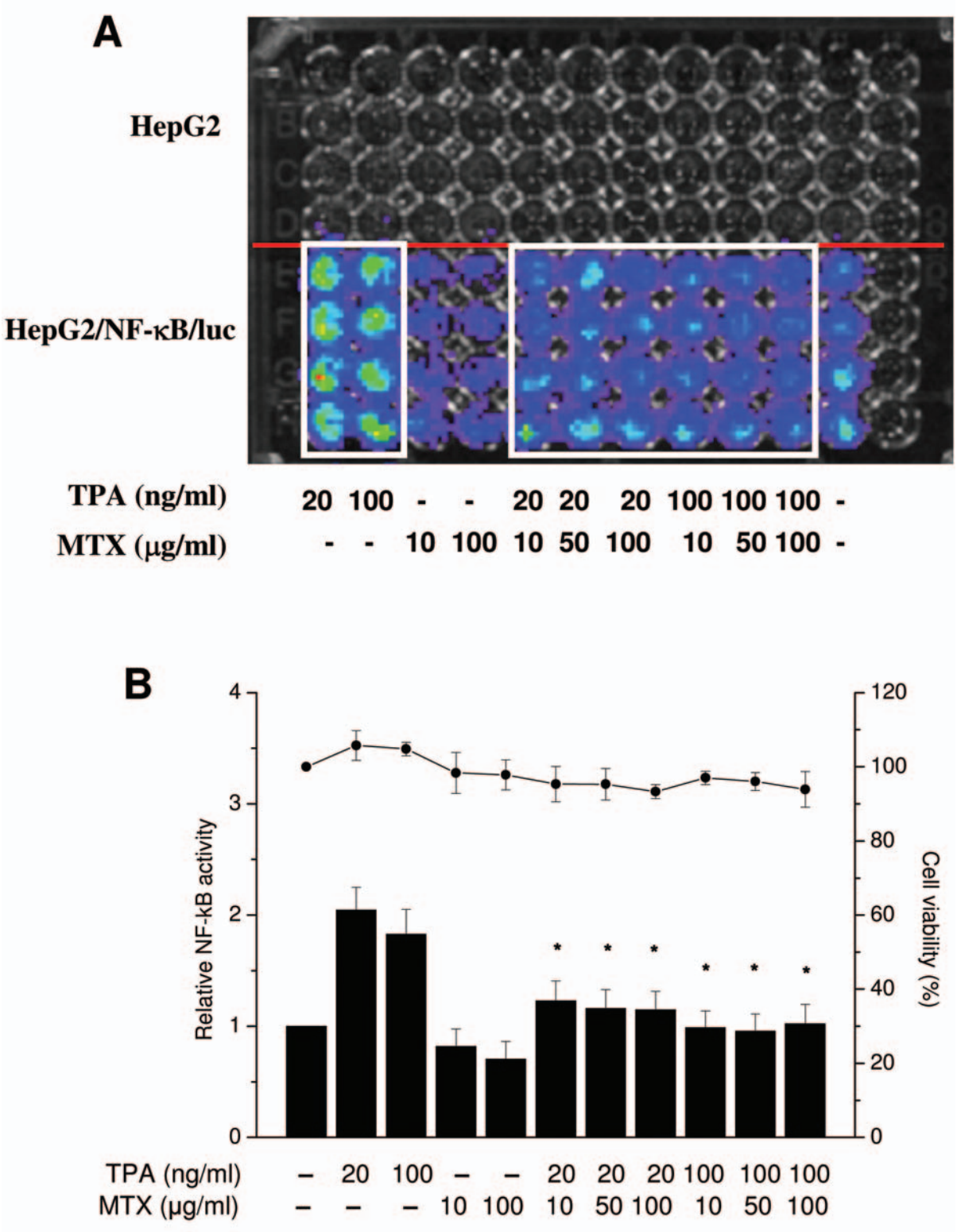

Figure 2. *Effect of methotrexate (MTX) on TPA-induced NF-κB activity in hepatoma cells. A, HepG2/NF-κB/Luc/L 5,000/cells were seeded into 96-well plates and treated with 20 ng/ml TPA and various doses of MTX for 16 h. B, The luciferase activity was determined by optical imaging after the addition of luciferin to the media. Effect of MTX on TPA-induced NF-κB activity was quantified at 16 h. The bars represent the relative luciferase activity (RLU), which is presented as the RLU relative to untreated cells. The lines represent the cell viability during treatment. Values are mean±standard error of three independent assays; *p<0.05 compared with the same TPA treatment and MTX untreated group.*

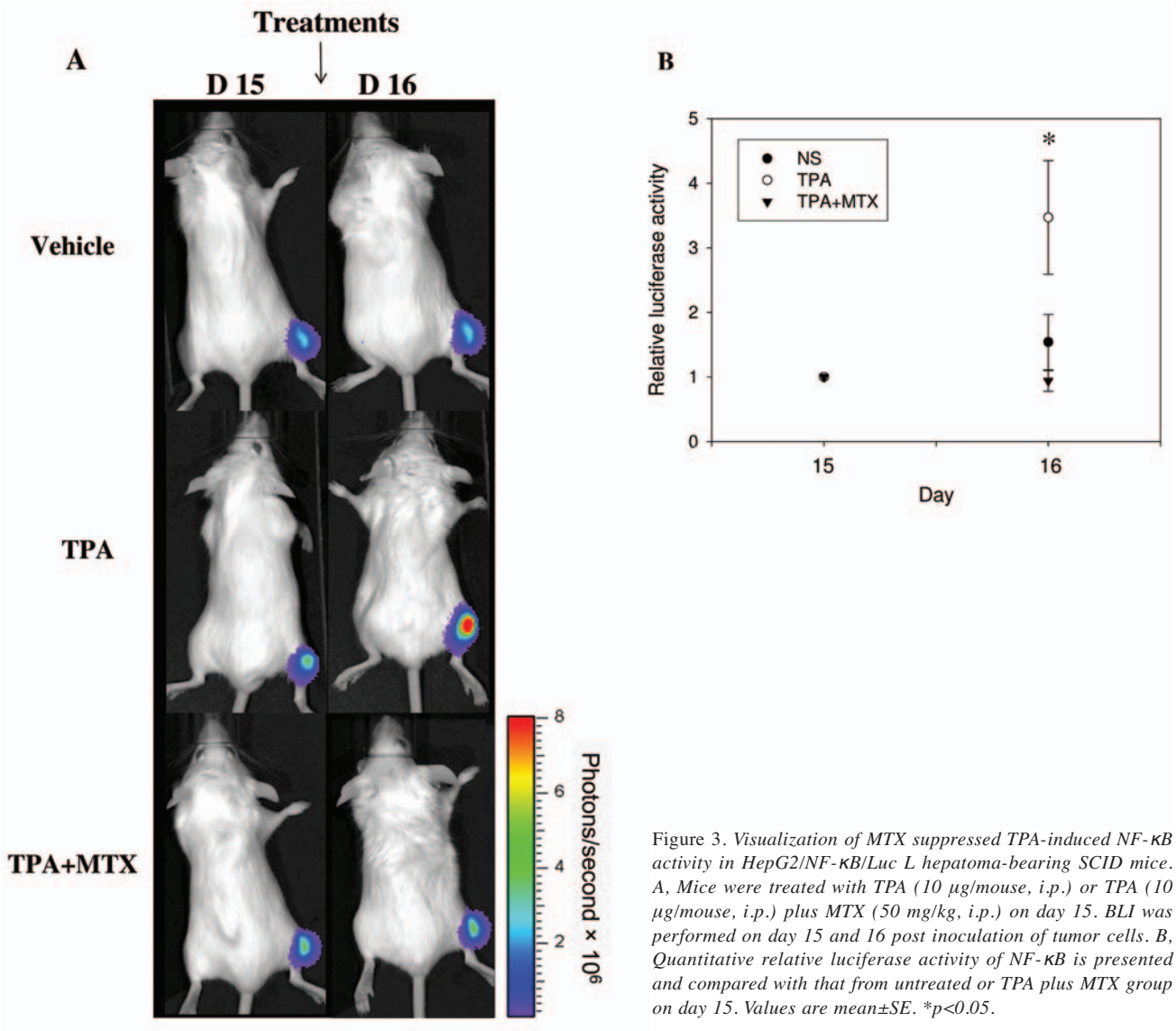

Figure 3. *Visualization of MTX suppressed TPA-induced NF-κB activity in HepG2/NF-κB/Luc L hepatoma-bearing SCID mice. A, Mice were treated with TPA (10 μg/mouse, i.p.) or TPA (10 μg/mouse, i.p.) plus MTX (50 mg/kg, i.p.) on day 15. BLI was performed on day 15 and 16 post inoculation of tumor cells. B, Quantitative relative luciferase activity of NF-κB is presented and compared with that from untreated or TPA plus MTX group on day 15. Values are mean±SE. *p<0.05.*

monitored the effect of TPA on the NF-κB activity in HepG2/NF-κB single clone cells by BLI at 16 h (Figure 2A). The quantitative results showed that relative NF-κB activity was increased 2.11-fold at 20 ng/ml TPA (Figure 2B) in HepG2/NF-κB/Luc/L cells. The results of relative NF-κB activity indicated 20 ng/ml of TPA was better than 100 ng/ml at inducing the activity of NF-κB.

The effects of MTX on TPA-induced NF-κB activity in HepG2/NF-κB/Luc cells were evaluated. The results showed that MTX (10, 50, 100 μg/ml) significantly ($p<0.05$) abolished the TPA (20, 100 ng/ml)-induced NF-κB activity at 16 h (Figure 2B). Although MTX suppressed TPA-induced NF-κB activity, the inhibition of endogenous NF-κB was not significant if HepG2/NF-κB/L cells were not treated with TPA. The cell viability was found to be unaffected by MTX (Figure 2B). Therefore, these results directly proved by BLI that MTX inhibited NF-κB activation. A highly responsive clone L for TPA-induced tumor promotion inhibited by MTX was selected for *in vivo* imaging study.

Monitoring MTX effects in vivo. The HepG2/NF-κB/Luc/L tumor cells containing the luciferase gene are driven by a promoter with five NF-κB-responsive elements in the hepatoma-bearing mice. Therefore, the luciferase activity reflected the NF-κB trans activity of HepG2/NF-κB/Luc/L tumor *in vivo*. The imaging data show that the bioluminescent signals from the TPA-treated group were

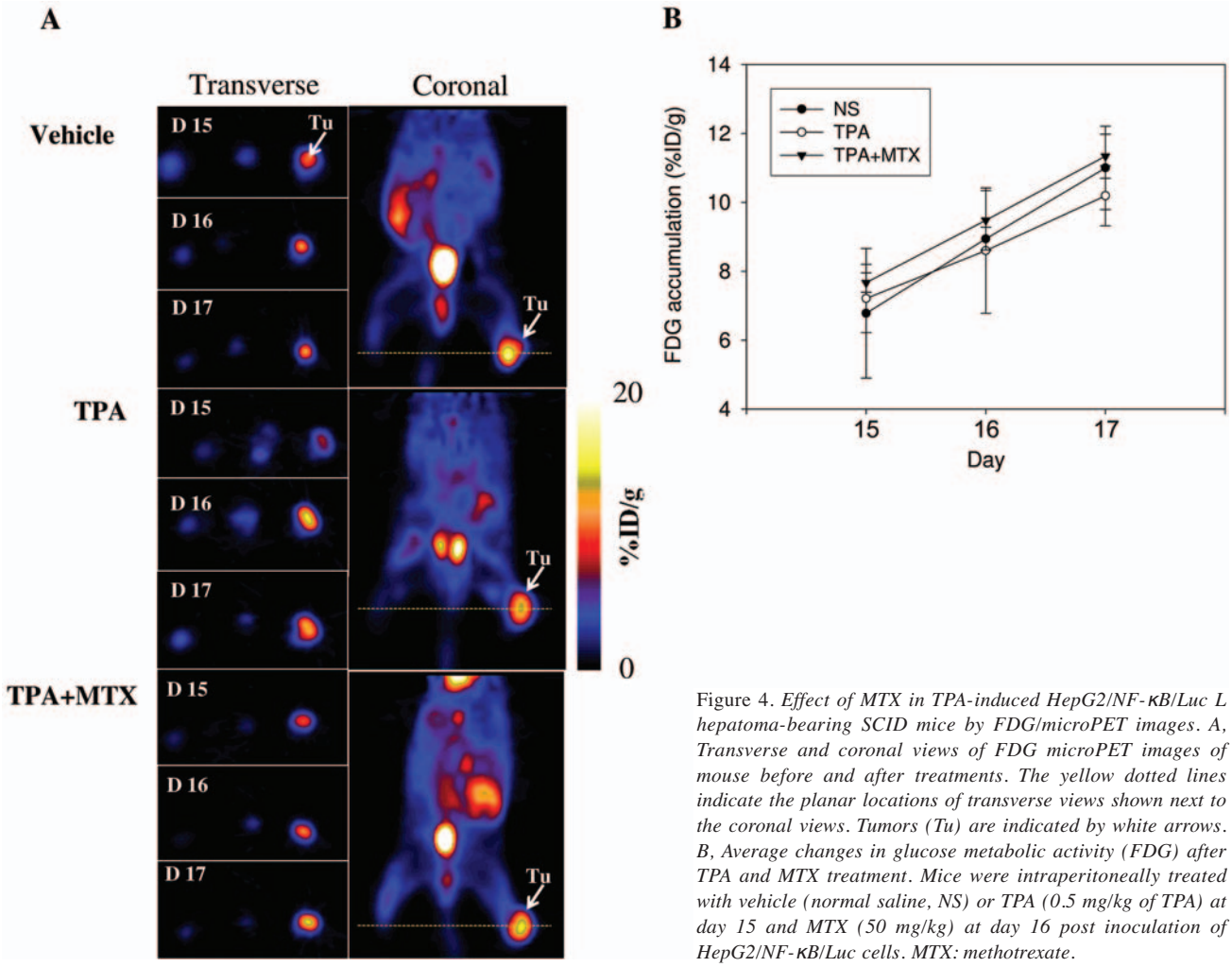

Figure 4. *Effect of MTX in TPA-induced HepG2/NF-κB/Luc L hepatoma-bearing SCID mice by FDG/microPET images. A, Transverse and coronal views of FDG microPET images of mouse before and after treatments. The yellow dotted lines indicate the planar locations of transverse views shown next to the coronal views. Tumors (Tu) are indicated by white arrows. B, Average changes in glucose metabolic activity (FDG) after TPA and MTX treatment. Mice were intraperitoneally treated with vehicle (normal saline, NS) or TPA (0.5 mg/kg of TPA) at day 15 and MTX (50 mg/kg) at day 16 post inoculation of HepG2/NF-κB/Luc cells. MTX: methotrexate.*

greater than those of TPA plus MTX and vehicle-treated mice (Figure 3A). The quantitative relative luciferase activity of TPA, TPA plus MTX, and the vehicle treated group was 0.94±0.16, 3.47±0.88, and 1.54±0.43, respectively (Figure 3B). The down-regulation of NF-κB activity was significant ($p<0.05$) in the TPA plus MTX treatment groups, compared with those from TPA-treated groups. These data indicated that the inhibition of NF-κB by MTX could be clearly monitored at 24 h after treatment *in vivo*.

FDG/MicroPET imaging. FDG/microPET imaging has been extensively used for diagnosing tumors that exhibit higher metabolic activity than normal tissues. To visualize glucose uptake in tumor xenografts before and after treatment, FDG/microPET imaging was performed. Compared to organs such as the heart, liver, kidneys, and bladder with endogenous FDG signals, the uptakes by tumors were significantly higher (Figure 4 A). The microPET imaging data showed that the FDG uptake by HepG2/NF-κB/Luc/L after TPA induction was not different from that of the vehicle group or the TPA plus MTX treatment group, which are quantitatively summarized in Figure 4B. It indicated that FDG/microPET imaging may not be able to demonstrate the metabolic outcome of tumor growth inhibition by MTX at 24 h after TPA induction.

Discussion

Because NF-κB plays a crucial role in tumor promotion, tumor cell survival and proliferation, NF-κB would be a potential target to suppress tumor growth by inhibition of its activity. The present study directly demonstrated the effect of MTX on TPA-induced NF-κB activity by BLI in living animals.

The effect of MTX in the regulation of NF-κB was satisfactorily monitored and analyzed by BLI *in vitro* (Figure 2). The experiments are in agreement with earlier *in vitro*

observation of MTX suppressing NF-κB activity (27). The antiproliferative effects of MTX were mediated by suppressing NF-κB activity through the inhibition of IκBα phophorylation and degradation (27). Furthermore, the dose of MTX was 50 mg/kg *in vivo*, which is below the maximum tolerance dosage (706 mg/kg *i.p.* bolus administration) (28). This might indicate that the change of NF-κB activity was not caused by the toxicity effect of MTX. Our results showed that noninvasive monitoring of the regulation of NF-κB activity correlated well *in vitro* and *in vivo*.

FDG/microPET was applied to monitor the therapeutic efficacy of MTX in a murine model of breast cancer (19). These mice were intravenously injected with MTX with 12 mg/kg at day 0, and FDG uptake was found to decrease markedly after treatment with MTX at day 7. However, the uptake of FDG did not show a significant change at day 1 after MTX administration (19). These results are consistent with the data in our present study. The change of glucose metabolism was not obvious after 24 h treatment with TPA and MTX, which might partly account for the fact that FDG uptake in HepG2/NF-κB/Luc/L tumors was not outstanding after one day's treatment (Figure 4). For the early detection of DNA proliferation, 3'-deoxy-3'-^{18}F-fluorothymidine (FLT) may have the potential to detect early changes in tumor proliferation after chemotherapy (29). Due to uptake by nucleotide transporter, FLT would be phosphorylated by thymidine kinase and retained in tumor cells (Figure 1). Furthermore, the influence of many physiological factors (angiogenesis, hypoxia, and inflammation) may have influence on the local FDG uptakes.

Optical imaging techniques represent a low cost and quick modality for real-time analysis of gene expression in small animal models but are limited by depth penetration and cannot easily be applied to humans (30). In contrast, radionuclide-based techniques have high sensitivity and good spatial resolution but are somewhat limited by their higher cost and production of isotopes. To date, various methodologies were developed for imaging the reporter gene expression in living cells and animals noninvasively and repetitively. Each of these modalities has unique applications, advantages and limitations that can be complementary to other modalities (31).

Noninvasive and sequential molecular imaging can serve as an accurate guide in diagnostic and therapeutic studies, since the tumor growth and therapeutic response in each animal can be immediately assessed rather than data from sacrificed animal at the same time points (32). Stathopoulos *et al*. investigated malignant pleural effusion (MPE) using NF-κB transfected green fluorescent protein-luciferase plasmid by BLI, and visualized the tumor lesions by combing the FDG/microPET/CT multi-modality (33). Their results demonstrated one of the applications of BLI and nuclear imaging in studying the effects of NF-κB in tumor progression and metastasis.

Drugs modulating NF-κB are needed for treatment in a number of diseases, including cancer. The hepatoma-bearing mouse model enabling *in vivo* imaging of luciferase reporter may be useful for screening potential drugs for the treatment of cancer during tumor promotion periods with aberrant NF-κB activation. Although the regulation of NF-κB has been studied by conventional techniques, the present study displays a rapid platform for the screening of anticancer drugs by BLI within 24 h. We propose that tumor models using other response elements or complete promoters may serve in a general approach to monitor gene expression *in vitro* and *in vivo* to study the mechanism of diseases and to screen exogenous factors, such as nutrients, Chinese herbs, pharmaceuticals, and environmental carcinogens for the modulation of gene expression and drug discovery.

Conclusion

The results described herein show that using the HepG2/NF-κB/L hepatoma cancer cells in conjugation with optical and FDG/microPET nuclear medical imaging platforms could be valuable, sensitive and specific imaging tools, particularly in drug discovery, and studies on tumorigenesis and metastasis.

References

1 Pikarsky E, Porat RM, Stein I, Abramovitch R, Amit S, Kasem S, Gutkovich-Pyest E, Urieli-Shoval S, Galun E and Ben-Neriah Y: NF-kappaB functions as a tumour promoter in inflammation-associated cancer. Nature *431*: 461-466, 2004.

2 Mantovani A: Cancer: inflammation by remote control. Nature *435*: 752-753, 2005.

3 Balkwill F and Coussens LM: Cancer: an inflammatory link. Nature *431*: 405-406, 2004.

4 Aggarwal BB, Shishodia S, Sandur SK, Pandey MK and Sethi G: Inflammation and cancer: how hot is the link? Biochem Pharmacol *72*: 1605-1621, 2006.

5 Ahmed KM, Cao N and Li JJ: HER-2 and NF-kappaB as the targets for therapy-resistant breast cancer. Anticancer Res *26*: 4235-4243, 2006.

6 Jin RJ, Lho Y, Connelly L, Wang Y, Yu X, Saint Jean L, Case TC, Ellwood-Yen K, Sawyers CL, Bhowmick NA, Blackwell TS, Yull FE and Matusik RJ: The nuclear factor-kappaB pathway controls the progression of prostate cancer to androgen-independent growth. Cancer Res *68*: 6762-6769, 2008.

7 Mattson MP and Meffert MK: Roles for NF-kappaB in nerve cell survival, plasticity, and disease. Cell Death Differ *13*: 852-860, 2006.

8 Roman-Blas JA and Jimenez SA: NF-kappaB as a potential therapeutic target in osteoarthritis and rheumatoid arthritis. Osteoarthritis Cartilage *14*: 839-848, 2006.

9 Mroz RM, Noparlik J, Chyczewska E, Braszko JJ and Holownia A: Molecular basis of chronic inflammation in lung diseases: new therapeutic approach. J Physiol Pharmacol *58(Suppl 5)*: 453-460, 2007.

10 Yan Y, Dalmasso G, Nguyen HT, Obertone TS, Charrier-Hisamuddin L, Sitaraman SV and Merlin D: Nuclear factor-kappaB is a critical mediator of Ste20-like proline-/alanine-rich kinase regulation in intestinal inflammation. Am J Pathol *173*: 1013-1028, 2008.
11 de Winther MP, Kanters E, Kraal G and Hofker MH: Nuclear factor kappaB signaling in atherogenesis. Arterioscler Thromb Vasc Biol *25*: 904-914, 2005.
12 Lernbecher T, Muller U and Wirth T: Distinct NF-kappa B/Rel transcription factors are responsible for tissue-specific and inducible gene activation. Nature *365*: 767-770, 1993.
13 Schmidt-Ullrich R, Memet S, Lilienbaum A, Feuillard J, Raphael M and Israel A: NF-kappaB activity in transgenic mice: developmental regulation and tissue specificity. Development *122*: 2117-2128, 1996.
14 Sizemore N, Leung S and Stark GR: Activation of phosphatidylinositol 3-kinase in response to interleukin-1 leads to phosphorylation and activation of the NF-kappaB p65/RelA subunit. Mol Cell Biol *19*: 4798-4805, 1999.
15 Jenkins DE, Oei Y, Hornig YS, Yu SF, Dusich J, Purchio T and Contag PR: Bioluminescent imaging (BLI) to improve and refine traditional murine models of tumor growth and metastasis. Clin Exp Metastasis *20*: 733-744, 2003.
16 Ho TY, Chen YS and Hsiang CY: Noninvasive nuclear factor-kappaB bioluminescence imaging for the assessment of host biomaterial interaction in transgenic mice. Biomaterials *28*: 4370-4377, 2007.
17 Sadikot RT and Blackwell TS: Bioluminescence imaging. Proc Am Thorac Soc *2*: 537-540, 511-532, 2005.
18 Medicherla S, Li L, Ma JY, Kapoun AM, Gaspar NJ, Liu YW, Mangadu R, O'Young G, Protter AA, Schreiner GF, Wong DH and Higgins LS: Antitumor activity of TGF-beta inhibitor is dependent on the microenvironment. Anticancer Res *27*: 4149-4157, 2007.
19 Aliaga A, Rousseau JA, Cadorette J, Croteau E, van Lier JE, Lecomte R and Benard F: A small animal positron-emission tomography study of the effect of chemotherapy and hormonal therapy on the uptake of 2-deoxy-2-^{18}F-fluoro-D-glucose in murine models of breast cancer. Mol Imaging Biol *9*: 144-150, 2007.
20 Plathow C and Weber WA: Tumor cell metabolism imaging. J Nucl Med *49(Suppl 2)*: 43S-63S, 2008.
21 Riemann B, Schafers KP, Schober O and Schafers M: Small animal PET in preclinical studies: opportunities and challenges. Q J Nucl Med Mol Imaging *52*: 215-221, 2008.
22 Taketani Y and Oka T: Tumor promoter 12-*O*-tetradecanoylphorbol-13-acetate, like epidermal growth factor, stimulates cell proliferation and inhibits differentiation of mouse mammary epithelial cells in culture. Proc Natl Acad Sci USA *80*: 1646-1649, 1983.
23 Hsiang CY, Wu SL and Ho TY: Morin inhibits 12-*O*-tetradecanoylphorbol-13-acetate-induced hepatocellular transformation *via* activator protein 1 signaling pathway and cell cycle progression. Biochem Pharmacol *69*: 1603-1611, 2005.
24 Iwase Y, Takemura Y, Ju-ichi M, Mukainaka T, Ichiishi E, Ito C, Furukawa H, Yano M, Tokuda H and Nishino H: Inhibitory effect of flavonoid derivatives on Epstein-Barr virus activation and two-stage carcinogenesis of skin tumors. Cancer Lett *173*: 105-109, 2001.
25 Nissen E, Pauli G and Vollenbroich D: WST-1 assay – a simple colorimetric method for virus titration. In Vitro Cell Dev Biol Anim *33*: 28-29, 1997.
26 Chang CH, Wang HE, Wu SY, Fan KH, Tsai TH, Lee TW, Chang SR, Liu RS, Chen CF, Chen CH and Fu YK: Comparative evaluation of FET and FDG for differentiating lung carcinoma from inflammation in mice. Anticancer Res *26*: 917-925, 2006.
27 Majumdar S and Aggarwal BB: Methotrexate suppresses NF-kappaB activation through inhibition of IkappaBalpha phosphorylation and degradation. J Immunol *167*: 2911-2920, 2001.
28 Lobo ED and Balthasar JP: Pharmacokinetic-pharmacodynamic modeling of methotrexate-induced toxicity in mice. J Pharm Sci *92*: 1654-1664, 2003.
29 Apisarnthanarax S, Alauddin MM, Mourtada F, Ariga H, Raju U, Mawlawi O, Han D, Bornmann WG, Ajani JA, Milas L, Gelovani JG and Chao KS: Early detection of chemoradioresponse in esophageal carcinoma by 3'-deoxy-3'-3H-fluorothymidine using preclinical tumor models. Clin Cancer Res *12*: 4590-4597, 2006.
30 Wu JC, Inubushi M, Sundaresan G, Schelbert HR and Gambhir SS: Optical imaging of cardiac reporter gene expression in living rats. Circulation *105*: 1631-1634, 2002.
31 Rudin M and Weissleder R: Molecular imaging in drug discovery and development. Nat Rev Drug Discov *2*: 123-131, 2003.
32 Minn AJ, Kang Y, Serganova I, Gupta GP, Giri DD, Doubrovin M, Ponomarev V, Gerald WL, Blasberg R and Massague J: Distinct organ-specific metastatic potential of individual breast cancer cells and primary tumors. J Clin Invest *115*: 44-55, 2005.
33 Stathopoulos GT, Zhu Z, Everhart MB, Kalomenidis I, Lawson WE, Bilaceroglu S, Peterson TE, Mitchell D, Yull FE, Light RW and Blackwell TS: Nuclear factor-kappaB affects tumor progression in a mouse model of malignant pleural effusion. Am J Respir Cell Mol Biol *34*: 142-150, 2006.

Received August 29, 2008
Revised December 2, 2008
Accepted February 13, 2009